Diagn Interv Radiol 2026; DOI: 10.4274/dir.2026.263921

MUSCULOSKELETAL IMAGING

ORIGINAL ARTICLE

Magnetic resonance imaging-based morphologic features associated with ankle sprain and increased risk of ligament tear

Hande Özen Atalay[1]
Gizem Timoçin Yığman[2]
Erol Erinç Dokuyucu[3]
Evrim Özmen[2]

[1]Hakkari State Hospital, Clinic of Radiology, Hakkari, Türkiye

[2]Koç University Faculty of Medicine, Department of Radiology, İstanbul, Türkiye

[3]Koç University Faculty of Medicine, İstanbul, Türkiye

PURPOSE

To identify magnetic resonance imaging (MRI)-based morphologic features of the distal tibiofibular syndesmosis and talocrural joint associated with ankle sprains and to determine which parameters are specifically linked to an increased risk of ligament tears after sprains.

METHODS

This retrospective study included ankle MRI examinations performed between January 2022 and November 2025. Two analytic datasets were constructed: Dataset 1 compared patients with ankle sprains and MRI-confirmed ligament tears to healthy controls with completely normal ankle MRIs; Dataset 2 compared controls, patients with sprains but no ligament tears, and patients with sprains and ligament tears. Standardized morphometric measurements of the distal tibiofibular syndesmosis and talocrural joint were obtained, including absolute and ratio-based parameters. Group comparisons were performed using appropriate univariable tests with multiple-comparison correction. Multivariable logistic regression was used to identify independent predictors of ligament tears. Inter-reader reliability was assessed using intraclass correlation coefficients and Bland–Altman analysis.

RESULTS

In Dataset 1, compared with healthy controls, tibiofibular clear space and the fibular notch depth–to–tibial thickness ratio were significantly higher in patients with ankle sprains and ligament tears, whereas the lateral malleolar height–to–talar articular width ratio was significantly lower (all $P < 0.05$). Multivariable analysis demonstrated that tibiofibular clear space and the fibular notch depth–to–tibial thickness ratio were independent predictors. In Dataset 2, tibiofibular clear space, fibular notch depth–to–tibial thickness ratio, and lateral malleolar height–to–talar articular width ratio differed significantly across three groups (all $P < 0.05$). Notably, only the lateral malleolar height–to–talar articular width ratio independently differentiated patients with sprains and ligament tears from those without tears ($P = 0.025$). Model discrimination was moderate to good (area under the curve: 0.699 and 0.785).

CONCLUSION

Specific MRI-based morphologic features are associated with both ankle sprain susceptibility and an increased risk of ligament tears. Among these, the lateral malleolar height–to–talar articular width ratio appears to be a morphometric parameter associated with an increased likelihood of ligament tears.

CLINICAL SIGNIFICANCE

MRI-based morphometric assessment, particularly the lateral malleolar height–to–talar articular width ratio, may help identify patients with ankle sprains who are at an increased risk for ligament tears and support more individualized clinical management.

KEYWORDS

Ankle joint, ankle sprain, ligament injury, magnetic resonance imaging, trauma

Corresponding author: Hande Özen Atalay

E-mail: handeozen15@gmail.com

Received 05 February 2026; revision requested 04 March 2026; last revision requested 04 April 2026; accepted 13 April 2026.

Epub: 05.05.2026

Publication date:

DOI: 10.4274/dir.2026.263921

You may cite this article as: Özen Atalay H, Timoçin Yığman G, Dokuyucu EE, Özmen E. Magnetic resonance imaging-based morphologic features associated with ankle sprain and increased risk of ligament tear. *Diagn Interv Radiol*. 05 May 2026 DOI: 10.4274/dir.2026.263921 [Epub Ahead of Print].

Lateral ankle sprain is among the most common musculoskeletal injuries in athletes, as well as in general populations, and represents a major source of morbidity worldwide.[1,2] The typical mechanism is forced inversion combined with internal rotation. It frequently occurs during sudden cutting or landing maneuvers, particularly in sports activities.[3,4] Despite being considered a relatively benign trauma, it is associated with high recurrence, chronic symptoms, and instability, eventually leading to long-term consequences such as post-traumatic osteoarthritis.[5]

Anatomical and biomechanical factors play an important role in the mechanism of ankle sprains. The ankle joint has a complex structure and limited osseous stability; therefore, its integrity depends on ligamentous structures.[6] The distal tibiofibular syndesmosis, in particular, contributes substantially to mortise stability; even minor widening of the syndesmosis can change joint mechanics and increase the risk of instability.[7] Additionally, variations in the talocrural joint have been shown to influence the susceptibility to lateral sprains, lateral malleolar fractures, or chronic instability.[8,9] In parallel, recent studies have demonstrated that chronic ankle instability is accompanied by functional changes that may be associated with underlying osseous morphology.[10]

Although several investigations have explored structural risk factors for ankle sprains, most prior studies have focused on either sprain history with ligament injury vs. non-sprain group (not a completely healthy control group) comparisons or on differentiating sprains from fractures.[8,11-16] Importantly, very few have incorporated a well-defined control group with completely normal magnetic resonance imaging (MRI), and previous research has rarely attempted to examine which morphological features increase the risk of sprains vs. those that contribute to the presence of ligament tears.

Thus, the specific MRI-based anatomical characteristics that either promote initial injuries or determine whether sprains evolve into ligament tears remain insufficiently understood. Identifying anatomical features associated with the presence of tears may have important clinical implications, including earlier risk stratification, targeted prevention strategies, and more individualized rehabilitation or treatment planning. To address this gap, this study aims to identify MRI-based morphological parameters of the distal tibiofibular syndesmosis and talocrural joint that are associated with ankle sprains and to determine which anatomical features are specifically linked to ligament tears.

Main points

- Distal tibiofibular syndesmosis and talocrural joint morphology show measurable differences on magnetic resonance imaging (MRI) in patients with ankle sprains and ligament tears.
- Tibiofibular clear space and the fibular notch depth–to–tibial thickness ratio is increased in patients with lateral ankle sprains.
- The lateral malleolar height–to–talar articular width ratio is the parameter that independently differentiates patients with sprains and ligament tears from those without tears.
- Detailed MRI-based morphometric assessment may improve anatomical risk stratification in patients with ankle sprains.

Methods

This retrospective study was conducted in accordance with the principles of the Declaration of Helsinki and was approved by the Koç University Biomedical Research Ethics Committee (approval number: 2025.503.IRB2.226, date: 10.11.2025). Written informed consent, including permission for the anonymized use of imaging data for research purposes, was obtained from all patients before radiologic evaluation as part of routine clinical practice at our institution.

Study participants

Patients who had an ankle MRI at Koç University Hospital, a tertiary care institution, between January 2022 and November 2025 were reviewed retrospectively. Individuals were included if the clinical referral or preliminary diagnosis indicated lateral ankle sprains or if their MRI reports contained terms such as "lateral ankle sprain" or "lateral ankle injury." A control group was formed from patients examined during the same period who had no history of ankle trauma in the MRI referral indications and whose MRI reports were interpreted as completely normal. Both pediatric and adult patients were eligible. Patients were excluded if they had a history of lower extremity surgery, fractures, tumors, infection, or marked degenerative joint disease. Additional exclusion criteria included injuries resulting from pronation–external rotation or pronation–abduction mechanisms, suboptimal MRI image quality, and cases with unclear or inconsistent trauma mechanisms. Based on these criteria, two analytic datasets were constructed: the first compared patients with ligament tears and sprains with healthy controls, and the second compared healthy controls, patients with sprains without ligament tears, and patients with sprains and ligament tears (Figure 1).

Magnetic resonance imaging protocol

MRI examinations were performed using a 3.0-T scanner (MAGNETOM Skyra; Siemens Healthineers, Erlangen, Germany) or a 1.5-T scanner (MAGNETOM Aera; Siemens Healthineers), with a dedicated 16-channel

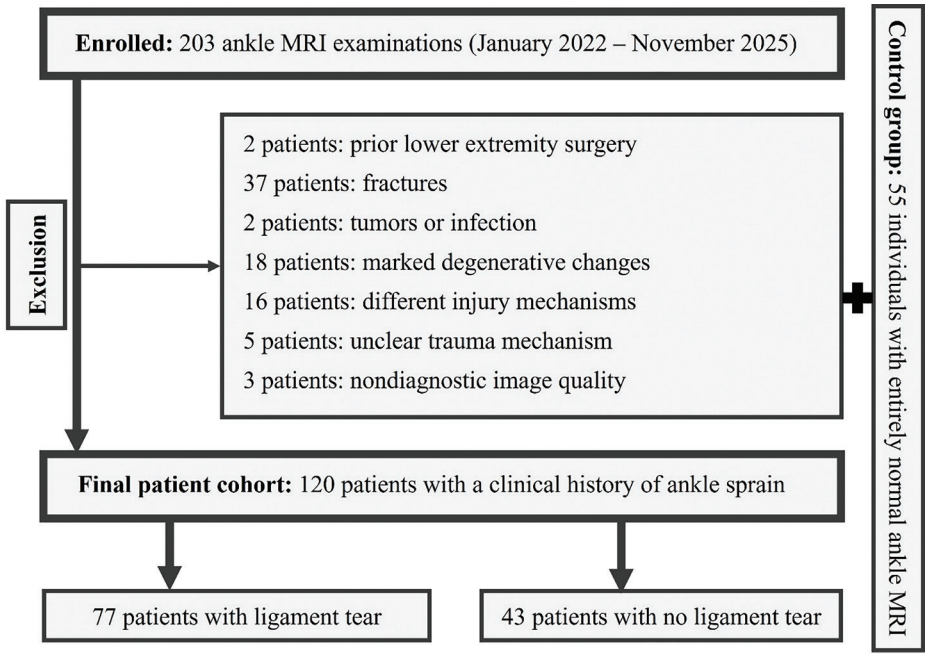

Figure 1. Flowchart of the study. MRI, magnetic resonance imaging.

phased-array coil optimized for high-resolution ankle imaging. Patients were positioned supine in a neutral position to avoid plantar flexion or dorsiflexion. The protocol included axial and sagittal T1-weighted spin-echo sequences, as well as axial, coronal, and sagittal fat-suppressed proton density sequences. In all cases, imaging was obtained on the same day or within a few days after the traumatic event and, therefore, generally reflects the acute phase of injuries.

Image analysis

All MRI examinations were independently reviewed by two radiologists with 10 and 15 years of experience, who were blinded to clinical details and patient groups. Morphometric MRI measurements included the angle between the anterior and the posterior facets, the anterior and posterior facet lengths of the fibular notch, the fibular notch depth, tibial and fibular thickness, medial and lateral malleolar articular surface heights, talar articular surface width, the length of the tibial incisura, the anterior and posterior widths of the tibiofibular syndesmosis, and the tibiofibular clear space (Figures 2 and 3). As described in previous morphometric MRI studies, axial measurements of the distal tibiofibular syndesmosis were obtained from images acquired approximately 10 mm above the tibial subchondral bone and parallel to the tibial plafond, where the anterior tibial tubercle and the fibular incisura are most clearly defined.[17] The line for the length of the tibial incisura was drawn tangentially

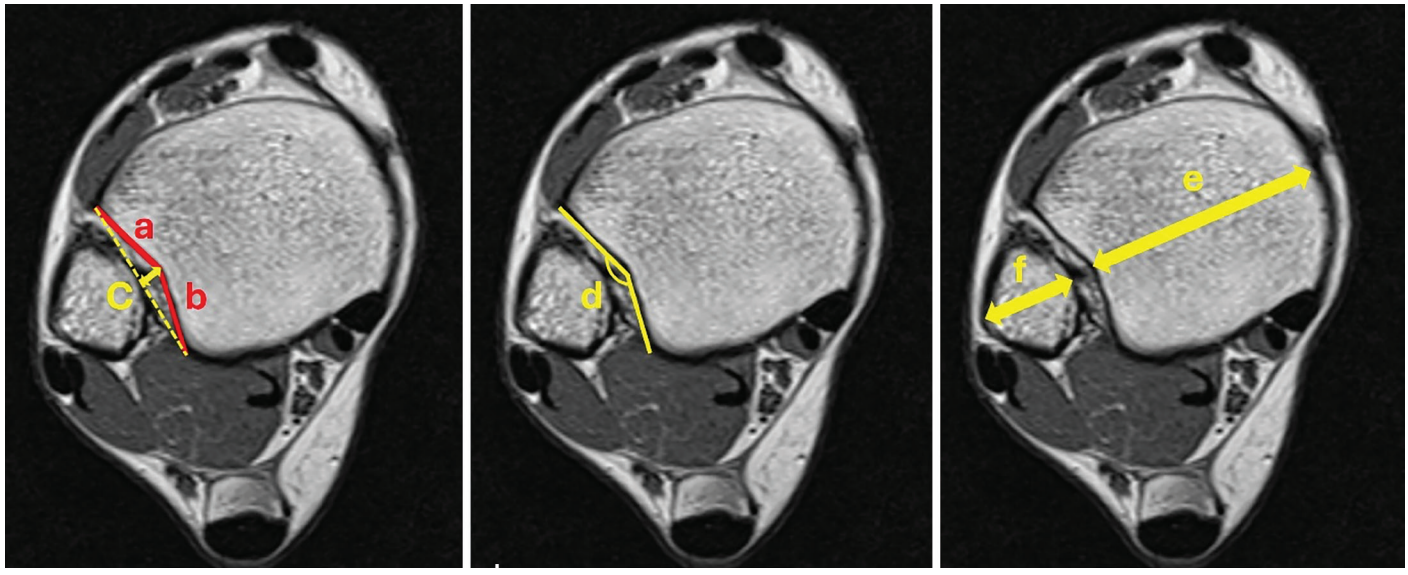

Figure 2. Magnetic resonance imaging (MRI)-based morphometric measurements of the distal tibiofibular syndesmosis. Axial MRI images demonstrating morphometric measurements: **(a)** anterior facet length, **(b)** posterior facet length, **(c)** fibular notch depth, **(d)** angle between the anterior and posterior facets, **(e)** tibial thickness, and **(f)** fibular thickness.

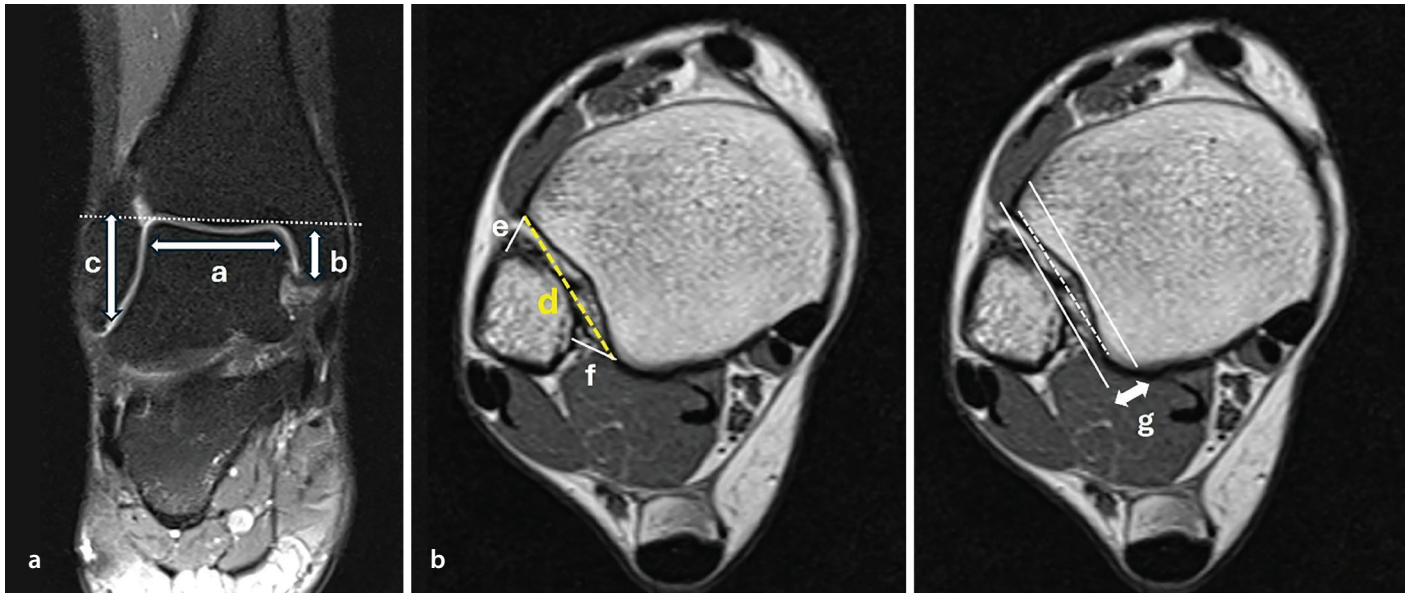

Figure 3. Magnetic resonance imaging (MRI)-based morphometric measurements of the ankle. Coronal and axial MRI images demonstrating morphometric measurements: **(a)** talar articular surface width, **(b)** medial malleolar articular surface height, **(c)** lateral malleolar articular surface height, **(d)** length of the tibial incisura, **(e)** anterior width of the tibiofibular syndesmosis, **(f)** posterior width of the tibiofibular syndesmosis, and **(g)** tibiofibular clear space.

between the most prominent portions of the anterior and posterior tibial tubercles. Using this reference, the anterior and posterior widths of the tibiofibular syndesmosis were measured from the intersections of this line with the tibial tubercles to the closest point of the fibula. The tibiofibular clear space was defined as the true distance between the fibula and the deepest point of the tibial incisura. Coronal measurements of the talocrural joint were obtained at the level where the talar articular surface was maximally visualized. A reference line parallel to the superior cortical surface of the talus was first drawn, along which the talar articular surface width was measured. The lateral and medial malleolar articular surface heights were then measured as the perpendicular distances from this reference line to the distal margins of the respective malleoli.

In addition to these absolute measurements, ratio-based parameters were calculated to normalize for inter-individual variations. These included the anterior-to-posterior facet length ratio, the lateral malleolar height–to–talar articular width ratio, the fibular notch depth–to–tibial thickness ratio, the fibular notch depth–to–fibular thickness ratio, the medial malleolar articular surface height–to–talar articular surface width ratio, the lateral malleolar articular surface height–to–medial malleolar articular surface ratio, and the ratio of the anterior width of the tibiofibular syndesmosis to the posterior width. Ligament tears include injuries of the anterior talofibular ligament (ATFL), the posterior talofibular ligament, and the deltoid ligament. Additionally, incidental talar dome osteochondral defects (OCDs) were noted. Ligament injuries were evaluated based on standard MRI criteria: Grade 1 injuries, representing ligament sprains without fiber disruption, were classified as sprains, whereas grade 2 (partial tears) and grade 3 (complete tears) injuries were categorized as ligament tears for the statistical analysis. All measurements were first performed independently by both radiologists, and these independent readings were used to assess inter-reader agreement. Subsequently, the measurements were jointly reviewed, and consensus values were determined for each case, which were then used for the statistical analyses.

Statistical analysis

All statistical analyses were performed using IBM SPSS Statistics (version 28.0; IBM Corp., Armonk, NY, USA). Normality was assessed using the Shapiro–Wilk test. Group comparisons in Dataset 1 were performed using the Mann–Whitney U test or Student's t-test for continuous variables and chi-square or Fisher's exact tests for categorical variables. Primary and exploratory parameters were evaluated using raw *P* values and false discovery rate (FDR)–adjusted q values to account for multiple testing. A multivariable logistic regression model was used to identify independent predictors of ligament tears, adjusting for age, sex, and laterality, and results were reported as odds ratios with 95% confidence intervals (CIs). Model performance was quantified using the receiver operating characteristic (ROC) the area under curve (AUC). In Dataset 2, differences among controls, patients with sprains only, and patients with sprains and ligament tears were evaluated using the Kruskal–Wallis test, followed by Holm-adjusted pairwise comparisons. A separate binary logistic regression model was applied to identify predictors of ligament tears among patients with sprains. For parameters that remained significant in multivariable analysis, optimal cut-off values were determined using ROC analysis based on the Youden index (sensitivity + specificity − 1). The Youden index was used to identify statistically optimal thresholds; however, clinical application may prioritize sensitivity or specificity depending on the clinical context. For all analyses, a P value < 0.05 was considered statistically significant.

Inter-reader agreement for morphometric measurements was assessed using the intraclass correlation coefficient (ICC) [two-way random model, absolute agreement; ICC (2,1)]. Given the distributional characteristics of ratio-based parameters, CIs were estimated using bootstrap resampling with 2,000 iterations. Bland–Altman analysis was additionally performed to investigate the acceptable interval for the inter-reader differences.

Results

A total of 203 ankle MRI examinations with a preliminary diagnosis of lateral ankle sprains, or with a report including terms such as "lateral ankle sprain" or "lateral ankle injury," performed between January 2022 and November 2025, were initially reviewed. Of these, 2 patients with prior lower extremity surgery, 37 with fractures, 2 with tumors or infection, 18 with marked degenerative changes, 16 with pronation–external rotation or pronation–abduction injury mechanisms, 5 with unclear trauma mechanisms, and 3 with non-diagnostic trauma were excluded according to the predefined criteria. The final study cohort consisted of 120 patients with a clinical history of ankle sprains. Among these, 77 patients (64.2%) had ligament tears, which were confirmed by MRI, whereas 43 patients (35.8%) had no ligament tears. Additionally, 55 individuals with entirely normal ankle MRIs were included as a control group.

The mean age of the cohort was 37.1 years (median: 38 years). Among all groups, 98 patients (56.0%) were women and 77 (44.0%) were men. The sprained or evaluated side was the left ankle in 70 patients (40.0%) and the right ankle in 105 patients (60.0%). No bilateral examinations were included. The mean age was 38.2 years (median: 41 years) in the group with ligament tears, 37.7 years (median: 38 years) in the group with sprains without tears, and 35.2 years (median: 34 years) in the control group. Sex distribution was 46 women and 31 men in the group with ligament tears, 24 women and 19 men in the group with sprains without tears, and 28 women and 27 men in the control group. Baseline comparisons demonstrated no significant differences between groups in terms of age or sex distribution ($P > 0.05$).

Among the 120 patients with ankle sprains, ATFL tears were the most common injury type and were identified in 73 patients (60.8%). Posterior talofibular ligament tears were noted in 10 patients (8.3%), and deltoid ligament tears were identified in 20 patients (16.7%). All patients with deltoid ligament tears also had concomitant lateral ligament tears, and no isolated deltoid ligament tears were observed. Additionally, four patients had grade 1 OCD, 3 patients had grade 2, and 3 patients had grade 3.

Patients with lateral ankle sprains and ligament tears vs. healthy controls

Dataset 1 compared patients with ankle sprains and MRI-confirmed ligament tears with healthy individuals who had entirely normal ankle MRIs to identify morphological features associated with ligamentous injuries. In this dataset, patients with ankle sprains and MRI-confirmed ligament tears demonstrated significantly greater tibiofibular clear space than the controls ($P = 0.005$). The fibular notch depth–to–tibial thickness ratio was significantly higher and the lateral malleolar height–to–talar articular width ratio was significantly lower in the group with ligament tears than in the healthy controls ($P = 0.034$ and $P = 0.019$, respectively) (Table 1). Among exploratory variables, several parameters reflecting distal tibiofibular morphology showed FDR-significant differences. The anterior and posterior widths of the ti-

biofibular syndesmosis, as well as the lateral-to-medial malleolar height ratio, were significantly greater in the group with sprains and ligament tears than in the healthy controls. Conversely, the medial malleolar articular surface height and the medial malleolar height–to–talar width ratio were significantly lower in the group with sprains and ligament tears than in the healthy controls (Table 2).

In the multivariable logistic regression model for Dataset 1, tibiofibular clear space remained a strong and statistically significant predictor ($P = 0.004$), with greater values independently associated with lateral ankle sprains and ligament tears. The fibular notch depth–to–tibial thickness ratio also demonstrated an independent association ($P < 0.001$). The lateral malleolar height–to–talar articular width ratio showed a borderline association after covariate adjustment ($P = 0.046$). The overall performance of the final model was good; the AUC was 0.785, indicating good discriminatory ability.

ROC analysis was additionally performed to identify optimal thresholds for the parameters that remained significant in multivariable analysis. For the tibiofibular clear space, a cut-off value of 4.3 mm yielded 66% sensitivity and 67% specificity for discriminating ankles with tears from controls (AUC: 0.644).

Table 1. Primary morphometric parameters (Dataset 1): comparison of patients with ligament tear vs. healthy controls

Parameter	Healthy controls	Ligament tear group	Difference	Test	*P* value
	Median (IQR)	Median (IQR)			
Tibiofibular clear space (mm)	4.1 (3.7–4.6)	4.6 (4.0–5.3)	+0.50 higher	MWU	**0.005**
Fibular notch depth–to–tibial thickness ratio	0.094 (0.074–0.117)	0.107 (0.084–0.131)	+0.0116 higher	t-test	**0.034**
Lateral malleolar height–to–talar width ratio	0.866 (0.798–0.969)	0.833 (0.763–0.917)	−0.0469 lower	t-test	**0.019**
Anterior-to-posterior facet length ratio	0.845 (0.614–1.176)	0.794 (0.613–1.100)	No significant difference	MWU	0.773
Angle between anterior and posterior facets (°)	134.9 (128.8–142.8)	133.6 (127.2–142.5)	No significant difference	MWU	0.780

IQR, interquartile range; MWU, Mann–Whitney U.

Table 2. Exploratory morphometric parameters (Dataset 1): multiple-comparison–adjusted analysis (FDR corrected)

Parameter	Healthy controls	Ligament tear group	FDR q value	Effect
	Median (IQR)	Median (IQR)		
Medial malleolar articular surface height (mm)	11.2 (9.6–12.9)	9.3 (7.4–10.9)	**1.7×10^{-5}**	Lower
Anterior width of tibiofibular syndesmosis (mm)	2.0 (1.7–2.5)	2.5 (1.9–3.2)	**0.0148**	Higher
Posterior width of tibiofibular syndesmosis (mm)	4.2 (3.9–4.8)	5.2 (4.7–5.8)	**2.0×10^{-6}**	Higher
Medial malleolar height–to–talar width ratio	0.433 (0.363–0.493)	0.358 (0.307–0.416)	**2.0×10^{-6}**	Lower
Lateral-to-medial malleolar height ratio	1.985 (1.809–2.345)	2.384 (1.991–3.015)	**2.74×10^{-4}**	Higher
Anterior facet length of fibular notch (mm)	10.1 (8.8–11.9)	10.1 (8.7–12.4)	ns	-
Posterior facet length of fibular notch (mm)	12.0 (10.1–13.5)	12.5 (10.8–14.3)	ns	-
Fibular notch depth (mm)	3.5 (2.8–4.5)	3.9 (3.3–4.8)	ns	-
Tibial thickness (mm)	38.0 (35.0–41.0)	36.8 (35.1–40.1)	ns	-
Fibular thickness (mm)	12.8 (11.9–13.9)	13.1 (11.9–14.4)	ns	-
Lateral malleolar articular surface height (mm)	22.6 (21.2–23.5)	21.7 (19.9–23.0)	ns	-
Talar articular surface width (mm)	25.9 (23.2–28.4)	26.0 (23.9–28.4)	ns	-
Length of tibial incisura (mm)	21.1 (19.6–22.9)	22.0 (19.8–24.3)	ns	-

ns, non-significant; FDR, false discovery rate; IQR, interquartile range.

For the fibular notch depth–to–tibial thickness ratio, the optimal threshold was 0.099, yielding 60% sensitivity and 58% specificity, although its discriminatory performance was limited (AUC: 0.609).

Healthy controls vs. patients with sprains without ligament tears vs. patients with sprains with ligament tears

Dataset 2 was used to evaluate differences between three groups (healthy controls, patients with sprains without ligament tears, and patients with sprains and tears) and to identify parameters linked to both sprain susceptibility and an increased risk of ligament tears after sprains. In this evaluation, significant differences were observed for tibiofibular clear space (P = 0.021), the fibular notch depth–to–tibial thickness ratio (P = 0.044), and the lateral malleolar height–to–talar articular width ratio (P = 0.012) (Table 3). For the tibiofibular clear space, post-hoc comparisons demonstrated a significant difference between controls and the group with ligament tears (Holm-adjusted P = 0.0143), whereas no significant differences were observed between controls and patients with sprains without tears or between those with sprains without tears and those with sprains and tears. Also, for the lateral malleolar height–to–talar articular width ratio, a significant difference was observed between patients with sprains without tears and those with sprains and tears (Holm-adjusted P = 0.0209), whereas comparisons involving the control group were not significant; this is more consistent with an increased risk of tears rather than sprain susceptibility. No significant differences were observed for the remaining primary parameters. Among exploratory variables, several demonstrated robust groupwise differences after FDR correction, many of which exhibited graded changes from controls to patients with sprains without tears and finally to patients with sprains and tears (Table 4).

In the logistic regression model restricted to patients with ankle sprains, the lateral malleolar height–to–talar articular width ratio was the only independent predictor of ligament tears (P = 0.025), whereas other parameters did not reach significance (P > 0.05). The discriminatory performance of the model was moderate, with an AUC of 0.699. ROC analysis further identified an optimal threshold for the lateral malleolar height–to–talar articular width ratio. A cut-off value of ≤ 0.86 was associated with an increased likelihood of ligament tears among patients with sprains, yielding a sensitivity of 62% and a specificity of 65% according to the Youden index–based threshold.

Table 3. Primary morphometric parameters (Dataset 2): Comparison among controls, patients with sprains without ligament tears, and patients with sprains with ligament tears

Parameter	Control	Sprain without tear	Sprain with tear	*P* value	Holm-adjusted pairwise results
	Median (IQR)	Median (IQR)	Median (IQR)		
Tibiofibular clear space (mm)	4.1 (3.7–4.6)	4.3 (3.7–5.2)	4.6 (4.0–5.3)	**0.0217**	Control vs. tear+: 0.0143 Control vs. tear–: ns Tear– vs. tear+: ns
Fibular notch depth–to–tibial thickness ratio	0.094 (0.074–0.117)	0.110 (0.087–0.136)	0.107 (0.084–0.131)	0.0442	All pairwise ns
Lateral malleolar height–to–talar articular width ratio	0.866 (0.798–0.969)	0.906 (0.811–0.977)	0.833 (0.763–0.917)	**0.0126**	Tear– vs. tear+: 0.0209 Control vs. tear+: ns Control vs. tear–: ns
Anterior-to-posterior facet length ratio	0.845 (0.614–1.176)	0.877 (0.691–1.194)	0.794 (0.613–1.100)	0.6499	All pairwise ns
Angle between anterior and posterior facets (°)	134.9 (128.8–142.8)	134.4 (124.8–143.3)	133.6 (127.2–142.5)	0.8043	All pairwise ns

ns, non-significant; IQR, interquartile range.

Table 4. Exploratory morphometric parameters (Dataset 2): FDR-corrected comparison among the three groups

Parameter	Control	Sprain without tear	Sprain with tear	FDR q value	Pattern/effect direction
	Median (IQR)	Median (IQR)	Median (IQR)		
Posterior width of the tibiofibular syndesmosis (mm)	4.2 (3.9–4.8)	4.7 (4.3–5.5)	5.2 (4.7–5.8)	**0.000009**	Monotonic ↑ (Control < tear– < tear+)
Medial malleolar height–to–talar width ratio	0.433 (0.363–0.493)	0.346 (0.316–0.418)	0.358 (0.307–0.416)	**0.000012**	Lower in sprain groups
Lateral-to-medial malleolar height ratio	1.985 (1.809–2.345)	2.417 (2.233–2.880)	2.384 (1.991–3.015)	**0.000061**	Higher in sprain groups
Medial malleolar articular surface height (mm)	11.2 (9.6–12.9)	8.9 (7.7–11.4)	9.3 (7.4–10.9)	**0.000076**	Lower in sprain groups
Lateral malleolar articular surface height (mm)	22.6 (21.2–23.5)	23.1 (21.2–24.8)	21.7 (19.9–23.0)	**0.0271**	Higher in sprain groups
Anterior width of the tibiofibular syndesmosis (mm)	2.0 (1.7–2.5)	2.3 (1.7–2.7)	2.5 (1.9–3.2)	**0.0348**	Monotonic ↑ (Control < tear– < tear+)
Other variables	-	-	-	ns	No pattern

ns: non-significant; FDR: false discovery rate; IQR, interquartile range.

Inter-reader reliability

Inter-reader agreement for morphometric measurements ranged from fair to good. The highest agreement was observed for the fibular notch depth–to–tibial thickness ratio, with an ICC of 0.77 (95% CI: 0.70–0.83). Tibiofibular clear space demonstrated moderate agreement (ICC: 0.65, 95% CI: 0.53–0.74), whereas the angle between the anterior and posterior facets showed good agreement (ICC: 0.72, 95% CI: 0.55–0.88). The anterior-to-posterior facet length ratio exhibited moderate agreement (ICC: 0.58, 95% CI: 0.41–0.71). In contrast, the lateral malleolar height–to–talar articular width ratio showed lower inter-reader agreement (ICC: 0.27, 95% CI: 0.18–0.37). Bland–Altman analyses demonstrated good agreement for the anterior-to-posterior facet length ratio and the fibular notch depth–to–tibial thickness ratio, whereas the lateral malleolar height–to–talar articular width ratio showed a small systematic bias with wider inter-reader variability (Figures 4 and 5).

Discussion

In this study, we systematically evaluated distal tibiofibular and talocrural joint morphology on MRI to determine which anatomical features increase the risk of ankle sprains and which parameters are specifically associated with an increased risk of ligament tears. Unlike previous research that typically examined either sprain-vs.-control differences or post-injury structural variations in isolation, our study incorporated a well-defined three-group design, allowing both sprain-related and tear-related features to be identified within the same analytical framework. Across datasets, tibiofibular clear space and the fibular notch depth–to–tibial thickness ratio emerged as consistently elevated in patients with ligament tears, indicating a broader syndesmotic openness and deepening that characterize ankles with confirmed tears (Figure 6). Most notably, the lateral malleolar height–to–talar width ratio distinguished tear risk, highlighting a lateral talocrural configuration that appears specifically relevant to an increased risk of tears rather than sprain susceptibility alone (Figure 7). In addition, several exploratory parameters related to syndesmotic width and malleolar geometry—including anterior and posterior tibiofibular syndesmotic width, the lateral-to-medial malleolar height ratio, medial malleolar articular surface height, and the medial malleolar height–to–talar width ratio—also demonstrated FDR-significant differences. These findings further support the presence of structural differences in distal tibiofibular configuration among patients with ligament tears.

Several of our findings are supported by prior MRI-based morphometric studies investigating distal tibiofibular and talocrural anatomy in lateral ankle instability. Vieira et al.[11] demonstrated that syndesmotic geometry and malleolar–talar relationships play a critical role in ankle sprain susceptibility, reporting significant alterations in fibular notch–related ratios and malleolar parameters in patients with sprains. Similarly, Ataoğlu et al.[15] showed that variations in anterior and posterior facet lengths, tibial thickness, and fibular notch–based ratios were associated with arthroscopically proven ankle instability. Our findings are in line with these observations, particularly with respect to the fibular notch depth–to–tibial thickness ratio and lateral malleolar height–to–talar width ratios, supporting the concept that reduced osseous containment predisposes the ankle to instability. However, important distinctions differentiate our study from these earlier works. Both Vieira et al.[11] and Ataoğlu et al.[15] primarily focused on comparing patients with unstable or sprain-positive ankles to control groups, without stratifying patients according to ligament integrity. By separately analyzing patients with sprains with and without MRI-confirmed ligament tears, our study extends this framework and demonstrates that although several morphometric parameters are already altered in

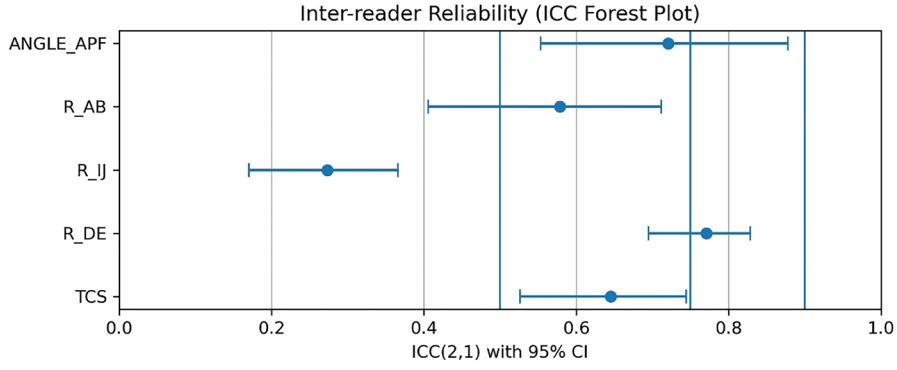

Figure 4. Inter-reader reliability analysis. ICC, intraclass correlation coefficient; CI, confidence interval; ANGLE_APF, angle between anterior and posterior facets; R-AB, anterior-to-posterior facet length ratio; R-IJ, lateral malleolar height to talar articular width ratio; R-DE, fibular notch depth to tibial thickness ratio; TCS, tibiofibular clear space.

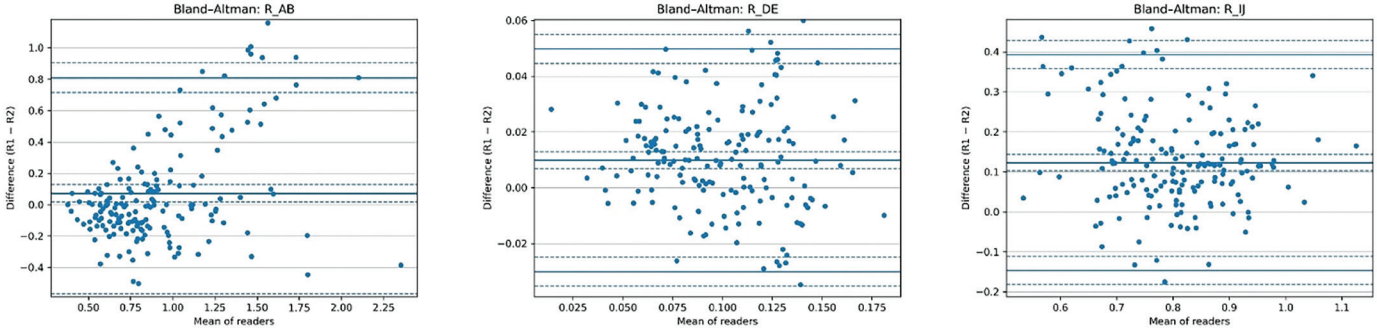

Figure 5. Bland–Altman plots for ratio-based measurement. R-AB, anterior-to-posterior facet length ratio; R-DE, fibular notch depth to tibial thickness ratio; R-IJ, lateral malleolar height to talar articular width ratio.

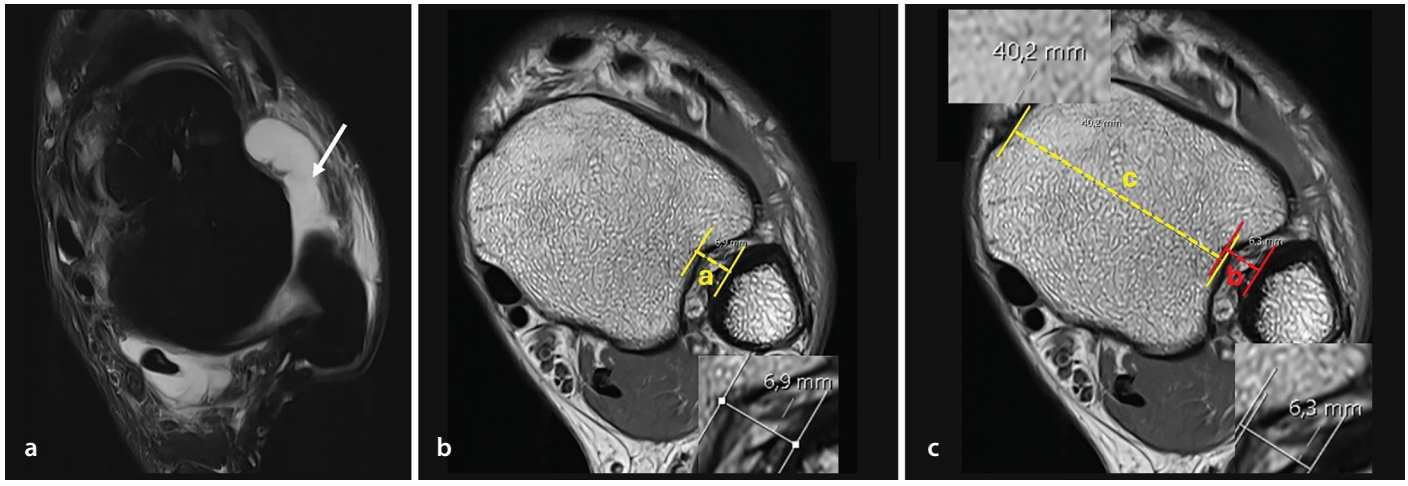

Figure 6. Axial ankle magnetic resonance imaging of a 48-year-old patient presenting with an ankle sprain demonstrates a complete tear of the anterior talofibular ligament (arrow in **Figure 6a**). Quantitative morphometric assessment (**Figure 6b** and **6c**) shows an increased tibiofibular clear space (**a**: 6.9 mm), exceeding the identified cut-off value of 4.3 mm. Additionally, the fibular notch depth **(b)**–to–tibial thickness **(c)** ratio is elevated (0.15), surpassing the threshold value of 0.099.

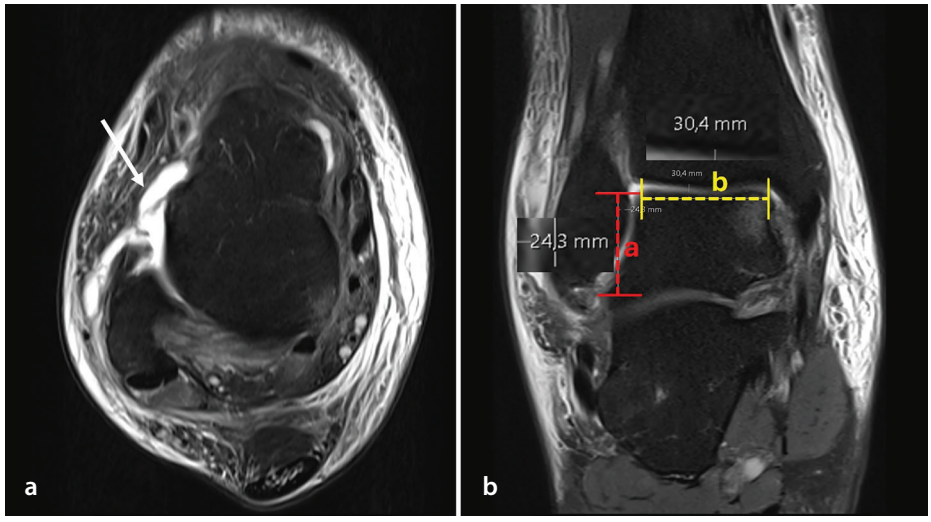

Figure 7. Axial and coronal ankle magnetic resonance imaging of a 46-year-old man presenting with an ankle sprain demonstrates a tear of the anterior talofibular ligament (arrow in **Figure 7a**). Morphometric analysis (**Figure 7b**) reveals a decreased lateral malleolar height **(a)**–to–talar articular width **(b)** ratio of 0.79, which falls below the identified cut-off value (≤ 0.86) associated with an increased likelihood of ligament tears.

patients with sprains, only a subset—most notably the lateral malleolar height–to–talar articular width ratio—is independently associated with a ligament tear rather than a sprain alone. Additionally, our inclusion of tibiofibular clear space and anterior–posterior syndesmotic width measurements provided further insight into syndesmotic openness, parameters that were not evaluated in prior studies.

In another study, Lee et al.[8] reported that the medial malleolar length–to–talar width ratio was associated with lateral ankle fractures in the ankle injury group. In our study, however, we found that lateral malleolar–related measurements demonstrated significant groupwise differences and showed changes from controls to injured groups. Unlike Lee et al.,[8] whose analysis primarily focused on the presence of sprains and ligament tears, our study further evaluated progression within injured patients. In this context, we identified the lateral malleolar height–to–talar articular width ratio as a specific discriminator of an increased risk of tears rather than sprain susceptibility alone.

Fibular position and syndesmotic configuration have been increasingly recognized as key contributors to ankle instability. Prior works have demonstrated that altered fibular positioning is associated with lateral ankle instability.[13,16] For example, Berkowitz and Kim[13] reported that a more posteriorly positioned fibula within the ankle mortise was significantly more common in patients undergoing lateral ankle stabilization procedures, suggesting that fibular malposition may be associated with an increased risk of chronic ankle instability. Also, Liu et al.[16] showed that specific shapes of the distal tibiofibular syndesmosis, particularly a shallow incisura, were associated with an increased risk of recurrent lateral ankle sprains. Although these studies primarily relied on qualitative classification or positional assessment, our work extends this concept by quantitatively integrating syndesmotic width, fibular notch depth, and ratio-based morphometric parameters within a unified analytical framework. In our cohort, fibular notch depth–related ratios were significantly increased in patients with ligament tears, supporting the role of syndesmotic openness and reduced fibular containment in ligament failure.

Although most primary morphometric parameters demonstrated good to moderate inter-reader agreement, the lateral malleolar height–to–talar articular width ratio showed comparatively lower ICC values in this study. This finding likely reflects the composite nature of this parameter, which may be influenced by slice selection variability. In contrast, other parameters rely on more sharply defined boundaries, resulting in higher reproducibility. Importantly, despite lower reproducibility, consensus measurements still demonstrated that the lateral malleolar height–to–talar articular width ratio emerges as an independent predictor of ligament tears in multivariable analyses. For improved standardization and to facilitate potential clinical application in future studies, we describe the measurement approach in detail.

On coronal MRIs, a reference line was first drawn parallel to the superior cortical surface of the talus at the level where the talar articular surface was maximally visualized. The talar articular width was measured along this line. On the same slice, the lateral malleolar articular height was measured as the perpendicular distance from this reference line to the distal tip of the lateral malleolus. The inferior boundary of the measurement corresponded to the level where the talofibular ligament originates from the fibula. All measurements were initially performed independently by two radiologists for inter-reader reliability analysis, and the values used for the final statistical analyses were obtained through consensus.

An additional consideration when interpreting our findings is the potential influence of post-traumatic changes on certain morphometric measurements. Parameters reflecting syndesmotic width, especially tibiofibular clear space, may partially represent secondary widening related to ligament disruption rather than purely predisposing anatomical configurations. In contrast, fibular notch depth–related measurements or the lateral malleolar height–to–talar articular width ratio represent geometric relationships between bony structures. Furthermore, the observation that the lateral malleolar height–to–talar articular width ratio differentiates patients with sprains and ligament tears from those without tears supports its potential role as a predisposing anatomical factor rather than solely a consequence of trauma.

This study has several limitations. First, it has a retrospective design and was performed at a single institution. However, the sample size was considered adequate for the regression analyses. Second, MRI examinations were performed on both 1.5-T and 3.0-T scanners. Although the same routine institutional protocol was used, this may still have introduced technical variability. However, as the evaluated parameters primarily represent osseous morphometric measurements, substantial effects of field strength differences on these measurements are unlikely. Third, the healthy control group includes individuals with entirely normal ankle MRIs, but no long-term clinical follow-up was performed. Therefore, we cannot definitively confirm that none of these individuals would later sustain an ankle sprain. Fourth, our study did not include clinical information such as activity levels or dynamic/weight-bearing assessments, which may have provided additional insights. Neurological conditions that could predispose patients to ankle sprains were not systematically evaluated due to the retrospective design. In addition, further analysis according to partial vs. complete tears was not performed because of the limited sample size. Future studies with larger cohorts may help clarify this point. Another limitation is the inclusion of both pediatric and adult patients, which may introduce heterogeneity related to skeletal maturity and epiphyseal closure status. Although age was included as a covariate in the analyses, subgroup analyses according to maturity were not performed. Finally, although the cohort size was relatively large, subgroup analyses may have been underpowered to detect smaller effect sizes.

In conclusion, this study indicates that specific MRI-based morphologic features of the distal tibiofibular syndesmosis and talocrural joint are associated with both susceptibility to ankle sprains and an increased risk of ligament tears. From a clinical perspective, the identified morphometric parameters may represent different stages of structural predisposition and injury. The fibular notch depth–to–tibial thickness ratio appears to reflect an underlying anatomical predisposition related to reduced osseous containment of the distal tibiofibular joint. Tibiofibular clear space may partly represent secondary widening associated with ligament disruption and, therefore, may reflect structural changes in ankles with confirmed tears. Finally, the lateral malleolar height–to–talar articular width ratio, which independently differentiated patients with sprains and ligament tears from those without tears, may represent a transition indicator for increased susceptibility to ligament tears following a sprain. Although these parameters alone cannot determine clinical outcomes, together they provide complementary morphologic information that may help improve structural risk stratification. Reporting markedly abnormal values may help identify patients at higher risk of ligament tears following ankle sprains. However, the discriminatory performance of these morphologic parameters was moderate to good, and the findings should be interpreted cautiously until validated in independent cohorts. Future prospective studies incorporating clinical and functional outcomes are required to validate these findings and to confirm the clinical utility of these morphometric parameters in risk stratification and individualized management.

Conflict of interest disclosure

Evrim Özmen, MD, serves as Section Editor for Diagnostic and Interventional Radiology. She had no involvement in the peer review of this article and had no access to information regarding its peer review. The other authors declared no conflicts of interest.

References

1. Gribble PA, Bleakley CM, Caulfield BM, et al. Evidence review for the 2016 International Ankle Consortium consensus statement on the prevalence, impact and long-term consequences of lateral ankle sprains. *Br J Sports Med*. 2016;50(24):1496-1505. [Crossref]
2. Sharma S, Dhillon MS, Kumar P, Rajnish RK. Patterns and trends of foot and ankle injuries in olympic athletes: a systematic review and meta-analysis. *Indian J Orthop*. 2020;54(3):294-307. [Crossref]
3. Machado M, Amado P, Babulal J. Ankle instability – review and new trends. *J Orthop Trauma Rehabil*. 2021;28. [Crossref]
4. Hertel J. Functional anatomy, pathomechanics, and pathophysiology of lateral ankle instability. *J Athl Train*. 2002;37(4):364-375. [Crossref]
5. Kim H, Son SJ, Seeley MK, Hopkins JT. Altered movement biomechanics in chronic ankle instability, coper, and control groups: energy absorption and distribution implications. *J Athl Train*. 2019;54(6):708-717. Erratum in: *J Athl Train*. 2020;55(1):5. [Crossref]
6. Golanó P, Vega J, de Leeuw PA, et al. Anatomy of the ankle ligaments: a pictorial essay. *Knee Surg Sports Traumatol Arthrosc*. 2016;24(4):944-956. [Crossref]
7. Hermans JJ, Beumer A, de Jong TA, Kleinrensink GJ. Anatomy of the distal tibiofibular syndesmosis in adults: a pictorial essay with a multimodality approach. *J Anat*. 2010;217(6):633-645. [Crossref]
8. Lee KM, Chung CY, Sung KH, et al. Anatomical predisposition of the ankle joint for lateral sprain or lateral malleolar fracture evaluated by radiographic measurements. *Foot Ankle Int*. 2015;36(1):64-69. [Crossref]
9. Magerkurth O, Frigg A, Hintermann B, Dick W, Valderrabano V. Frontal and lateral characteristics of the osseous configuration in chronic ankle instability. *Br J Sports Med*. 2010;44(8):568-572. [Crossref]
10. Verhagen EALM, van der Beek AJ. Optimising ankle sprain prevention: a critical review and practical appraisal of the literature. *Br J Sports Med*. 2010;44(15):1082-1088 [Crossref]
11. Vieira J, Vieira AC, Vieira A. MRI analysis of distal tibiofibular joint and ankle anatomy to assess lateral ankle sprain risk. *Insights Imaging*. 2025;16(1):213. [Crossref]

12. Beynnon BD, Renström PA, Alosa DM, Baumhauer JF, Vacek PM. Ankle ligament injury risk factors: a prospective study of college athletes. *J Orthop Res*. 2001;19(2):213-220. [Crossref]
13. Berkowitz MJ, Kim DH. Fibular position in relation to lateral ankle instability. *Foot Ankle Int*. 2004;25(5):318-321. [Crossref]
14. Mason J, Kniewasser C, Hollander K, Zech A. Intrinsic risk factors for ankle sprain differ between male and female athletes: a systematic review and meta-analysis. *Sports Med Open*. 2022;8(1):139. [Crossref]
15. Ataoğlu MB, Tokgöz MA, Köktürk A, Ergişi Y, Hatipoğlu MY, Kanatlı U. Radiologic evaluation of the effect of distal tibiofibular joint anatomy on arthroscopically proven ankle instability. *Foot Ankle Int*. 2020;41(2):223-228. [Crossref]
16. Liu Q, Lin B, Guo Z, Ding Z, Lian K, Lin D. Shapes of distal tibiofibular syndesmosis are associated with risk of recurrent lateral ankle sprains. *Sci Rep*. 2017;7(1):6244. [Crossref]
17. Lepojärvi S, Niinimäki J, Pakarinen H, Leskelä HV. Rotational dynamics of the normal distal tibiofibular joint with weight-bearing computed tomography. *Foot Ankle Int*. 2016;37(6):627-635. [Crossref]